Electronic Supplementary Material (ESI) for Green Chemistry.

Electronic Supporting Information

A 3D-Printed Continuous Flow Platform for the Synthesis of Methylaluminoxane

Yirong Feng, Jie Wang, Haomiao Zhang*, Jingdai Wang, and Yongrong Yang

State Key Laboratory of Chemical Engineering, College of Chemical and Biological Engineering, Zhejiang University, 310027, P.R. China
E-mail: haomiaozhang@zju.edu.cn

1. Microdroplet generator

We assemble a microdroplet generator that can produce smaller droplets based on capillary tubes. A capillary tube with 160 μm O.D. (outer diameter) and 100 μm I.D. (inner diameter) is inserted into the 3D-printed T-junction through nuts and ferrules. In the other end, the capillary tube is inserted into and fixed in a PFA tubing with 250 μm I.D. By design, water flows through the capillary in the centre of the tubing, while toluene flows around it outside the capillary. Growing droplets detach when the forces exerted by the co-flowing continuous phase exceed the interfacial tension. In order to analyze the droplet size and distribution, we monitor and record the process of microdroplet generation in different flowrates with the high-speed camera. An image processing program (ImageJ) is used to extract the features of microbubbles from the recorded images, such as Sauter mean diameter d_{32}. The formed droplets are highly uniform in size for each flowrate, and the effect of flowrates on the microdroplet sizes is subsequently obtained. The size of microdroplets in the toluene−water mixer ranges from 160 to 400 μm while changing the flowrate of the continuous phase (toluene). However, the flowrate of the disperse phase (water) has negligible effect on the droplet size.

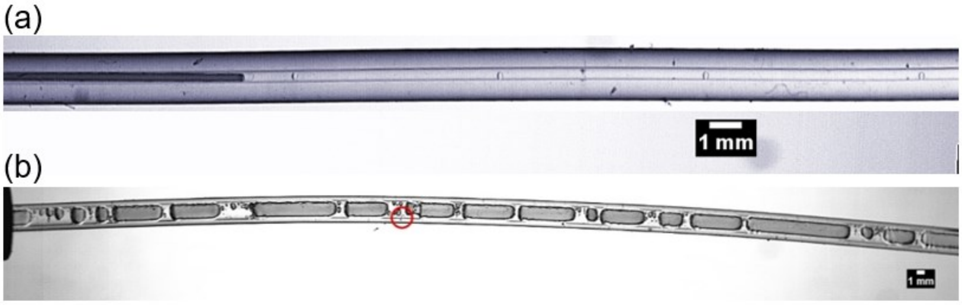

Fig. S1 (a) The recorded dispersion state of water droplets in toluene using customized microdroplet generator (flowrates: toluene 2 mL/min and water 30 μL/min) and (b) the hydrolytic reaction process occurred in the microchannel under water flowrate of 64 μL/min, toluene flowrate of 2.0 mL/min, and TMA/toluene flowrate of 6.0 mL/min with TMA mass fraction of 6.10 wt.% from the high-speed camera.

We conduct a hydrolytic reaction experiment, and record the reaction process at the outlet of the customized passive micromixer, as shown in Fig. S1. Most of water reacts immediately after the initial contact with TMA but minimal amount of water needs to react in the downstream of the microchannel. Furthermore, solids may form during the reaction due to excessive hydrolysis of TMA or MAO, which are of concern for processing as the gradual deposition of solids on walls can lead to increased pressure drops and ultimately microchannel clogging. Based on these aspects, we design a miniature continuous stirred-tank reactors cascade to reduce this process risk and get rid of the gas-liquid segmented flow pattern.

2. μCSTR module

The μCSTRs module (Fig. S2a-b) consists of six cylindrical chambers in series, which are connected to each other through 2mm channels attached tangentially to the bottom part of the chamber. By design, all reactor chambers are 3D printed as one unit without further manual construction. Each chamber has a diameter of 9 mm and depth of 5 mm (Fig. S2c). To avoid sharp corners for unexpected clogging, fillets are added inside each chamber and at the entrance and the exit of each chamber. We can open or block its upper part by installing commercial IDEX fittings/plugs. The multiphase mixture is efficiently blended by a magnetic stirring spheroid of 3 mm wide and 5 mm long which is powered and controlled by the magnetic force of a magnetic stirrer. With the stirrers inside each chamber and fittings connected, the total reactor volume of the μCSTRs (6 chambers) is 1.7 mL.

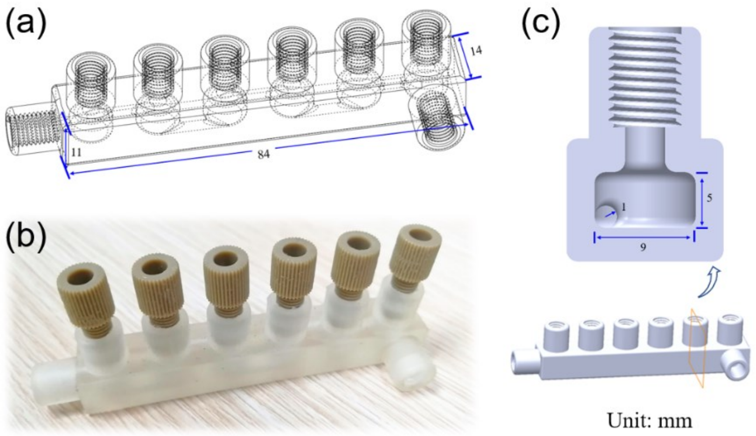

Fig. S2 (a) A transparent CAD file and (b) an image of the actual 3D-printed prototype showing the μCSTR module with fluidic inlets, ports for the magnetic stirrers, six chambers, and interconnections; (c) a cross-section view of the μCSTR chamber with key dimensions.

Subsequently, we measure the residence time distribution (RTD) profiles of the μCSTR module with 6-chambers in order to characterize the mixing performance using the pulse injection method. Fig. S3 shows the schematic of the RTD measurements. The carrier phase is deionized (DI) water that is delivered by a syringe pump. And a two position six-port switching valve (IDEX Health & Science LLC, MXP9900-000) is connected for tracer injection with a 12 μL sample loop. Brilliant Blue FCF is used as the tracer and its absorbance is integrated over the wavelength range of 600–650 nm to reduce noise in the signal. In-line UV-Vis spectroscopy (Ocean Optics, Inc., light source: DH-2000-BAL; spectrometer: FLAME-S-UV-VIS) combined with LabVIEW control is used to record and analyze the concentration profiles of the tracer at both the inlet and the outlet.

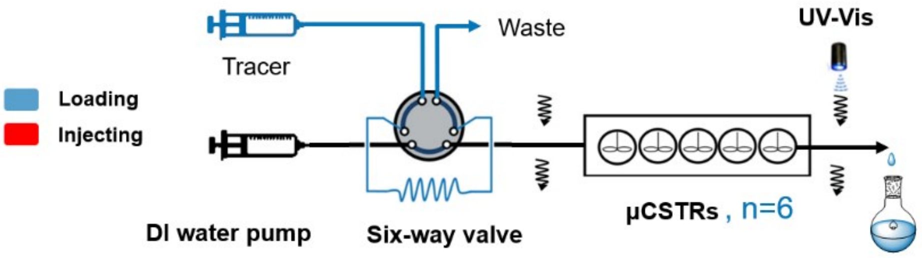

Fig. S3 Schematic of the residence time distribution (RTD) experiment using in-line UV-Vis to record concentration profiles at the inlet and the outlet.

The mixing performance of the μCSTR module is assessed by comparing the deconvoluted outlet concentration profile to the ideal CSTRs-in-series model (Eq. S1)[1, 2].

$$E(t) = \frac{t^{n-1}}{(n-1)!\tau^{n}} e^{-t/\tau} \qquad (S1)$$

Since the tracer pulse injected is not a perfect pulse, the outlet concentration profile is the convolution of the inlet concentration profile and RTD. Therefore, we extract the RTD from the inlet and outlet concentration profiles by regression with the exponentially modified Gaussian (EMG) distribution model (Eq. S2). A custom-developed MATLAB data processing program is utilized to obtain the RTD of measured and ideal CSTR-in-series model.

$$E(t) = \frac{\lambda}{2} exp\left(\frac{\lambda}{2}(2\mu + \lambda\sigma^{2} - 2t)\right) erfc\left(\frac{\mu + \lambda\sigma^{2} - t}{\sqrt{2}\sigma}\right) \qquad (S2)$$

We perform RTD measurements at constant flowrates of 1-20 mL/min and stirring speed of 600-1500 rpm, covering the conditions used for the synthesis of MAO. All results show high consistency between the ideal and measured RTD profiles (Fig. S4), depicting that dead volume in the reactor is negligible and there is sufficient agitation in each chamber to achieve rapid mixing.

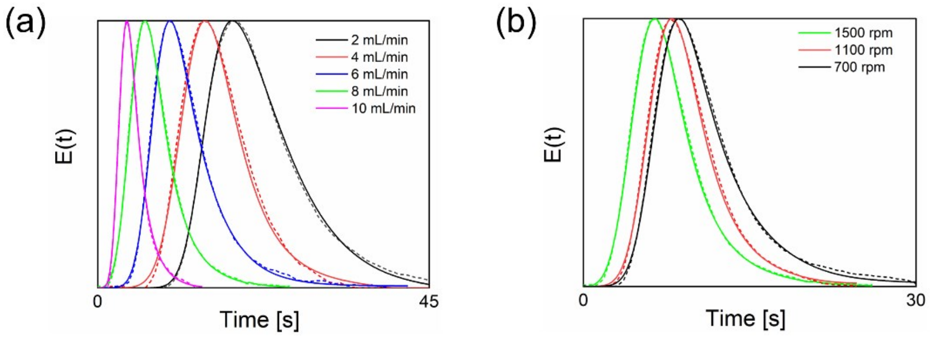

Fig. S4 RTD profiles of the 3D-printed μCSTR module with six chambers for influence of (a) flowrate at 1500 rpm and (b) stirring speed at 8 mL/min. Dashed lines denote experimental RTD profiles, and solid lines denote the profiles obtained from the ideal CSTRs-in-series model.

3. Particle size analysis

Our flow platform is capable of handling solid effectively. To provide insight into the risk of clogging, we measure the particle size distribution using a laser diffraction size analyzer (Malvern Mastersizer 2000, United Kingdom), and refer the equivalent diameter of equal volume sphere to the mean particle diameter. We repeat each group of samples three times for the average distribution curve. Specifically, Fig. S5 shows the particle size distribution of the solid by-product obtained from the experiment with flowrate of 6 mL/min, H_2O/Al of 0.8, and TMA mass fraction in toluene of 5.32 wt%. The mean particle size (245 μm) is much smaller than the narrowest characteristic length (2 mm, the diameter of the interconnection in the 3D-printed μCSTR module; 1.59 mm, the diameter of the microtubing), suggesting that our platform is suitable to long-term continuous processing of MAO synthesis.

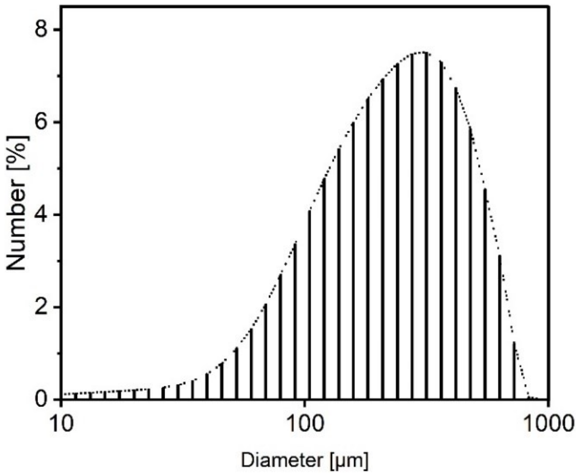

Fig. S5 Particle size distribution of the solid by-product obtained from the experiment with flowrate of 6 mL/min, H_2O/Al of 0.8, and TMA mass fraction in toluene of 5.32 wt%.

4. ^{1}H NMR spectra of MAO

To further illustrate the comparison between our synthesized i-MAO sample and the commercial c-MAO sample, we obtain the ^{1}H NMR spectra from both samples in toluene in a sealed NMR tube at 600 MHz on an Agilent DD2 (DirectDrive2) instrument, as shown in Fig. S6. The i-MAO sample investigated is prepared under H_2O/Al of 0.8 and TMA mass fraction in Toluene of 6.10 wt.%. THF-d_8 is added for field/frequency lock at a 4:1 v/v ratio of THF-d_8 to MAO solution. Addition of excess THF narrows the TMA resonance significantly and shifts the TMA resonance upfield. The obtained ^{1}H NMR spectra are referenced to signals of toluene (δ = 2.31 ppm). A broad signal at approximately δ ~ -0.15 to -1 ppm corresponds to the polymeric MAO structure and the sharp resonance of residual TMA at δ = -0.8 ppm. These NMR spectra indicate the two MAO samples are similar, without other impurities introduced.

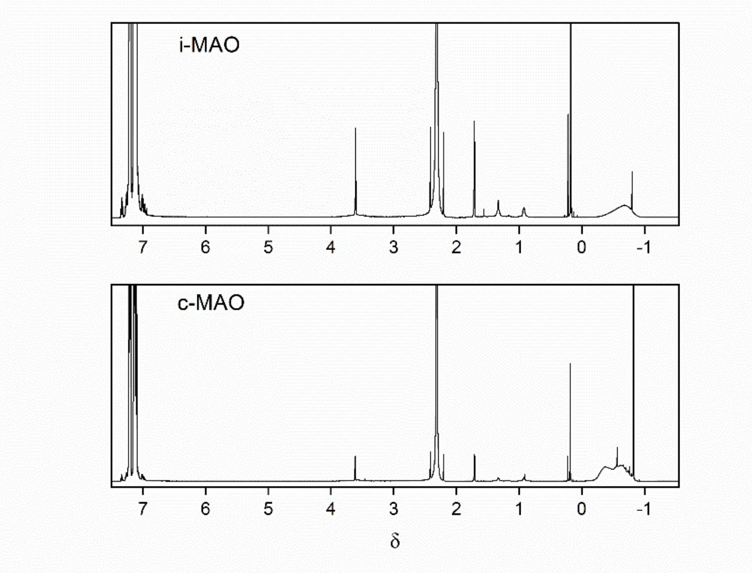

Fig.S6 ^{1}H NMR spectra of i-MAO and c-MAO in toluene.

5. Cocatalytic activity evaluation

5.1 Bis(imino)pyridine iron complexes as catalyst for ethylene oligomerization

Bis(imino)pyridine iron complexes in combination with MAO as catalysts exhibit excellent activity and linearity for α-olefin production. In this system, iron acetylacetonate ($Fe(acac)_3$) is mainly used as the iron source to form a homogeneous pre-catalyst with a 2,6-bis[1-(4-methoxy-2-methylphenylimino)ethyl]pyridine ligand (L) which is synthesized by reaction of 4-methoxy-2-methylaniline and 2,6-diacetylpyridine, as shown in Scheme S1. 4-methoxy-2-methylaniline is added to a solution of 2,6-diacetylpyridine in absolute ethanol. The solution is refluxed for 48 h after dropping a small amount of glacial acetic acid. Upon cooling to room temperature, the product is crystallized out from ethanol, and it is then filtered, washed with cold ethanol, and dried in a vacuum oven (60 ^oC) overnight. Then, the bis(imino)pyridine ligand is mixed with $Fe(acac)_3$ in identical molar ratio and dissolved in toluene, obtaining a homogeneous orange-red mixture solution, abbreviated as L-$Fe(acac)_3$. The concentration of the catalyst precursor in toluene, in terms of iron atoms, is 4 μmol/mL.

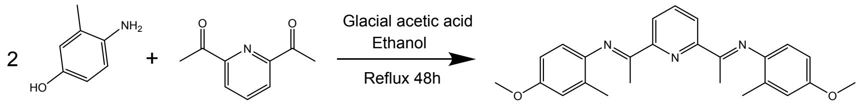

Scheme S1 Synthesis of 2,6-bis[1-(4-methoxy-2-methylphenylimino)ethyl]pyridine (L).

Ethylene oligomerization experiments are carried out in a 250 mL dried three-necked round-bottom flask which is immersed in a Magnetism Msier with an agitation speed of 800 rpm. A continuous and steady stream of ethylene is introduced into the flask under stirring. The desired amount of toluene (50 mL), MAO and L-Fe(acac)$_3$ (2 μmol) are sequentially added into the flask, of which the amount of MAO added is calculated based on a set Al/Fe molar ratio of 1000. The oligomerization is initiated immediately and lasts for 30 min at atmosphere pressure. Finally, the reaction is quenched by addition of the acidified ethanol solution. The product is then separated by filtration. The insoluble polyethylene wax is washed out and dried overnight at 60 °C under reduced pressure until a constant weight is achieved. For soluble oligomers, an internal standard (n-heptane, 1.0 mL) is injected into the liquid phase. α-olefin products are quantitatively analyzed by Agilent GC 6890 equipped with an Agilent HP-5 column (5% phenylmethylsiloxane, 30 m × 0.32 mm × 0.25 μm), and the temperature programming is: injection temp, 320^{o}C; initial column temperature, 50 ^{o}C/2 min; progress rate, 20 ^{o}C /min; final column temperature, 300 ^{o}C/10 min. The yield of volatile C_4 fraction is determined by extrapolation based on the α value, which is a characteristic coefficient of the Schulz-Flory distribution, as calculated from the relative rate of chain propagation and chain termination or the ratio of the molar amounts of two subsequent oligomer fractions, C_{14} and C_{12} in this case. Finally, the co-catalytic activity is quantitatively analyzed by summation of the amount of the linear α-olefin products, including the soluble oligomers and insoluble polymers.

5.2 Cp_2ZrCl_2 as catalyst for ethylene polymerization

Ethylene polymerization is conducted at 70 ^{o}C in a 250 mL dried three-necked round-bottom flask equipped with a magnetic stirred bar. Then, it is immersed in a Magnetism Msier with an agitation speed of 800 rpm. Ethylene is continuously fed into the solvent under stirring. In the next, 100 mL dry toluene is introduced into the flask, followed by the addition of the desired amount of MAO. The polymerization is initiated by addition of the catalyst Cp_2ZrCl_2

(15 μmol), in which the Al/Zr molar ratio is kept at 500. After the required polymerization time of 1 h, the system is quenched by addition of an acidified ethanol solution. The precipitated polymer is collected by filtration and washed out with methanol. The collected polymer is dried overnight under reduced pressure at 60 °C to obtain polyethylene in white powder for analysis of the co-catalytic activity of MAO.

5.3 Cocatalytic activity evaluation with less MAO

In widely accepted methods, metallocenes and transition metal complexes require large amounts of MAO to reach high activities. For instance, in order to compare with the commercially available MAO product, Okajima et al. employed their in-house prepared MAO as cocatalyst in propylene polymerization using zirconocene, titanocene, nickel, and iron catalysts at high ratios of aluminum to transition-metals on the order of 1000.[3] Hence, we start with polymerization test at excess amount of MAO to evaluate the cocatalytic activity.

In order to highlight the difference in depth, we conduct two groups of polymerization tests with significantly less MAO – 10 Al atoms per catalyst. Both polymerization processes remain the same as aforementioned except for the proportion of MAO in the catalyst. For ethylene oligomerization test, the desired amount of toluene (50 mL), MAO, and L-Fe(acac)$_3$ (0.3 mmol) is sequentially added into a flask, of which the amount of MAO is calculated based on an Al/Fe molar ratio of 10. For ethylene polymerization test, the desired amount of toluene (100 mL), MAO, and Cp_2ZrCl_2 (0.16 mmol) is sequentially added into a flask, of which the amount of MAO is calculated based on an Al/Zr molar ratio of 10. Specifications of our prepared MAO sample (i-MAO) and the commercial MAO sample (c-MAO) are nearly identical, and the performance comparison in polymerizations is listed in Tables S1-S2, respectively. Both results confirm that i-MAO performs similarly well compared to c-MAO for their co-catalytic activities and physical properties of the polymer products.

Table S1. Performance comparison of i-MAO and c-MAO in olefin polymerization with L-Fe(acac)$_3$ catalyst (Al/Fe=10; solvent: toluene, 50 mL; T=50 ^{o}C; P=1 bar; t=30 min).

Co-catalyst	Activity (kg (mol Fe)$^{-1}$h^{-1})
i-MAO	13.04
c-MAO	11.56

Table S2. Performance comparison of i-MAO and c-MAO in olefin polymerization with Cp_2ZrCl_2 catalyst (Al/Zr=10; solvent: toluene, 100 mL; T=70 ^{o}C; P=1 bar; t=60 min).

Co-catalyst	Activity (kg (mol Zr)$^{-1}$h^{-1})	Mw (10^4 g·mol^{-1})	PDI	T_m (^{o}C)
i-MAO	26.31	1.78	1.72	120.82
c-MAO	30.33	2.45	2.27	121.65

Reference

1. O. Levenspiel, *Chemical Reaction Engineering, 3rd ed.*, John Wiley & Sons, Inc, New York, 1999.
2. Y. Mo and K. F. Jensen, *React. Chem. Eng.*, 2016, **1**, 501-507.
3. Y. Okajima, Y. Nakayama, T. Shiono and R. Tanaka, *Eur. J. Inorg. Chem.*, 2019, 2392-2395.